

An 11-Mb/s 2.1-mW Synchronous Superregenerative Receiver at 2.4 GHz

F. Xavier Moncunill-Geniz, Pere Palà-Schönwälder, *Member, IEEE*, Catherine Dehollain, *Member, IEEE*, Norbert Joehl, and Michel Declercq, *Fellow, IEEE*

Abstract—This paper presents a low-voltage low-power high-speed superregenerative receiver operating in the 2.4-GHz industrial–scientific–medical band. The receiver uses an architecture in which, thanks to the presence of a phase-locked loop, the quench oscillator is operated synchronously with the received data at a quench frequency equal to the data rate. This mode of operation has several benefits. Firstly, the traditional problem of poor selectivity in this type of receiver is to a large extent overcome. Secondly, considerably higher data rates can be achieved than with classical receivers. Thirdly, the bit envelope can be matched to the superregenerative oscillator, which improves sensitivity. The receiver includes an RF front end optimized to support high quench frequencies at low supply voltages, responding to today's increasing demand for high speed and low power consumption. The prototype implemented is very simple and achieves a data rate of 11 Mb/s with a current consumption of 1.75 mA at a supply voltage of 1.2 V—an excellent tradeoff between cost, performance, and power consumption.

Index Terms—Low power, radio receiver, RF oscillator, superregenerative receiver.

I. INTRODUCTION

SUPERREGENERATIVE receivers are well suited to short-range wireless communications due to their exceptional simplicity, reduced cost, and low power consumption. Typical applications for this type of receiver are remote control systems (such as garage door openers, robots, model ships, airplanes, etc.), short distance telemetry, and wireless security [1]–[7]. The interest of industry in the superregenerative receiver is made evident by recent patent applications [8]–[10], more than eighty years after it was presented by Armstrong in 1922 [11]. Hence, superregenerative architectures are present today in commercial products, in which they typically operate at low data rates.¹ Research on superregeneration has been carried out in unlicensed RF bands up to millimeter-wave frequencies [12], [13]. However, only very recent papers report operation

in the 2.4-GHz industrial–scientific–medical (ISM) band [3], [5]–[7], [14], [15], which, compared to lower frequency bands, allows larger signal bandwidth to be used and is available worldwide.

It is well known that classical superregenerative receivers suffer from poor frequency selectivity when they are applied to narrowband communications and, consequently, are more vulnerable to noise and interference than other systems [2], [16]. This behavior is caused by the characteristic pulsating operation of the receiver, in which the superregenerative oscillator (SRO) controlled by the quench oscillator samples the envelope of the input signal asynchronously at a rate (quench frequency) that is considerably higher than the modulation bandwidth. During the sampling process, the SRO is sensitive to the input signal for a relatively small fraction of the quench period. Hence, the sensitivity periods are much shorter than the data period and, consequently, the RF bandwidth, which is inversely proportional to the duration of the sensitivity periods, becomes much larger than the modulation bandwidth.

The selectivity of a superregenerative receiver can be improved by decreasing the quench frequency. In practice, this limits its use to low data-rate applications. Although the selectivity can also be improved by using special quench wave shapes, the RF bandwidth will continue to be considerably larger than the modulation bandwidth [2]. The use of stable and high- Q frequency references such as surface acoustic wave (SAW) or bulk acoustic wave (BAW) devices can also decrease the reception bandwidth, although this unavoidably reduces the quench frequency and, therefore, the data rate [4], [16]. Significant improvements can be obtained by using smart Q -enhancement techniques, as reported recently in [5] and [6].

Responding to today's increasing demand for high-speed and low-power consumption, in this paper we present a superregenerative receiver prototype designed to support high quench frequencies. We also make use of a synchronous mode of operation, which has been successfully applied in spread-spectrum communications [14], [15] and yields significant advantages over conventional receivers. Thanks to the presence of a phase-locked loop (PLL), the SRO is quenched synchronously with the received data so that the quench frequency equals the data rate. The usefulness of this mode of operation is twofold: on the one hand, for a given data rate, the quench frequency can be reduced in comparison with a conventional receiver to obtain a more selective receiver with an RF bandwidth comparable to that of the input signal and, on the other, for a fixed quench frequency (e.g., limited by resonator Q), the synchronous operation allows higher data rates to be achieved. Receiver sensitivity

Manuscript received October 16, 2006. This work was supported by the Spanish Dirección General de Investigación under Grant TIC2003-02755 and Grant TEC2006-12687/TCM, and by the École Polytechnique Fédérale de Lausanne.

F. X. Moncunill-Geniz and P. Palà-Schönwälder are with the Department of Signal Theory and Communications, Technical University of Catalonia, 08034 Barcelona, Spain (e-mail: moncunill@tsc.upc.edu).

C. Dehollain, N. Joehl, and M. Declercq are with the Electronics Laboratory, Swiss Federal Institute of Technology, CH-1015 Lausanne, Switzerland (e-mail: catherine.dehollain@epfl.ch).

Digital Object Identifier 10.1109/TMTT.2007.896796

¹Telecontrolli Wireless Products—RF Receivers, Telecontrolli Srl, Casoria, Italy. [Online]. Available: <http://www.telecontrolli.com>

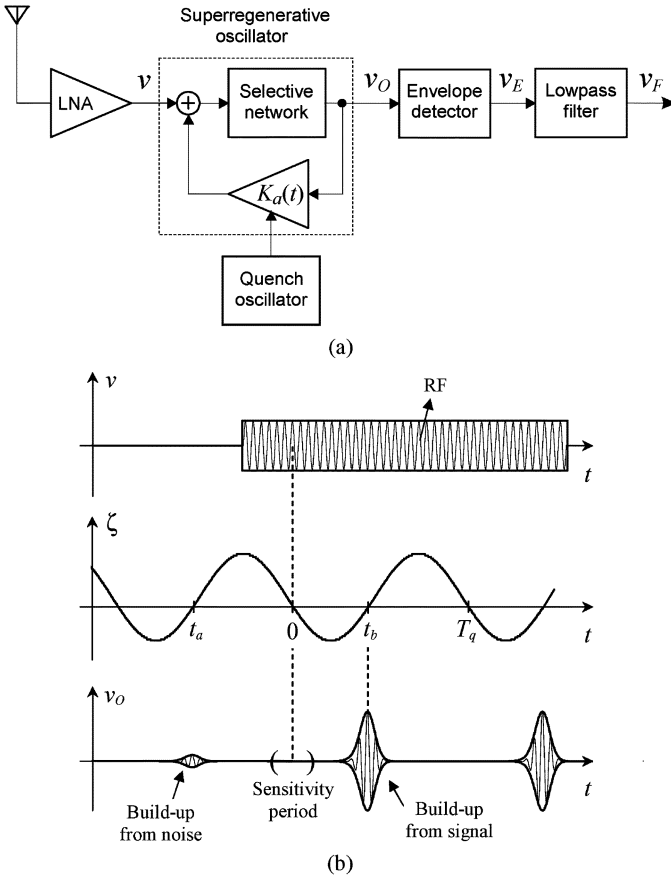


Fig. 1. (a) Block diagram of a conventional superregenerative receiver. (b) SRO RF input signal, closed-loop damping function, and output voltage in the linear mode of operation.

can also be improved when specially shaped symbols are transmitted.

In [17], the design of a superregenerative RF front end conceived to support high data rates is presented. The front end operates at 3 V of voltage supply and reaches 10 Mb/s. In this paper, we describe the entire receiver architecture and present an improved design in which the supply voltage has been decreased to 1.2 V and the transfer speed increased to 11 Mb/s. The design achieves very low consumed energy per bit (0.19 nJ/bit), thus offering excellent performance at low cost.

II. BASIC THEORY OF SUPERREGENERATION

The block diagram of a conventional narrowband superregenerative receiver is shown in Fig. 1(a). The core of the receiver is the SRO. It is an RF oscillator that is controlled by a low-frequency quench generator or quench oscillator, which causes the RF oscillations to rise and die out repeatedly. The signal generated in the SRO is composed of a series of RF pulses separated by the quench period T_q , in which the periodic buildup of the oscillations is controlled by the input signal $v(t)$, as depicted in Fig. 1(b).

In the linear mode of operation, the oscillations are damped before they reach their limiting equilibrium amplitude, and their peak amplitude is proportional to that of the injected signal. In

the logarithmic mode, the amplitude of the oscillations is allowed to reach its limiting equilibrium value, which is determined by the nonlinearity of the active devices. In this mode of operation, the amplitude of the RF pulses remains constant, but the incremental area under the envelope is proportional to the logarithm of the amplitude of $v(t)$ [3]. In both modes, the modulating input signal can be retrieved by low-pass filtering the envelope of the RF pulses, as depicted in Fig. 1(a). The low-noise amplifier (LNA) improves signal reception and minimizes SRO re-radiation through the antenna.

According to the analysis presented in [3], the SRO can be modeled as a frequency-selective network fed back through a variable-gain amplifier. Typically, the selective network has two dominant poles that provide a bandpass response centered on a certain frequency ω_0 , which is characterized by the transfer function

$$G(s) = K_0 \frac{2\zeta_0\omega_0 s}{s^2 + 2\zeta_0\omega_0 s + \omega_0^2} \quad (1)$$

where ζ_0 is the damping factor and K_0 is the maximum amplification. The feedback amplifier controlled by the quench oscillator provides a gain $K_a(t)$ that varies periodically with time. The closed-loop operation of the system can be characterized from the instantaneous damping factor, which is defined as

$$\zeta(t) = \zeta_0 (1 - K_0 K_a(t)). \quad (2)$$

In the periods in which $\zeta(t)$ is negative [see Fig. 1(b)], the system becomes unstable and the amplitude of the RF oscillation rises. When $\zeta(t)$ changes to positive, the system stabilizes and the oscillation is damped.

The behavior of the receiver can be characterized from its response to a single RF pulse applied within the limits defined by t_a and t_b in Fig. 1(b), which can be expressed as

$$v(t) = V p_b(t) \cos(\omega t + \phi) \quad (3)$$

where V is a positive value representing the peak amplitude and $p_b(t)$ is a normalized shaping function that equals zero outside the interval (t_a, t_b) . The voltage generated at the output of the SRO is another RF pulse that starts increasing at $t = 0$ (i.e., when $\zeta(t)$ crosses zero with a negative slope) and achieves the maximum amplitude at $t = t_b$ (i.e., at the zero crossing of $\zeta(t)$ with a positive slope). The expression of the output pulse within the interval $(0, T_q)$ is [3]

$$v_O(t) = V K |H(\omega)| p(t) \cos(\omega_0 t + \phi + \angle H(\omega)) \quad (4)$$

where K is an amplification factor, $H(\omega)$ is a normalized bandpass frequency-response function centered on ω_0 , and $p(t)$ is the normalized output pulse envelope. K , $H(\omega)$, and $p(t)$ are mainly determined by the frequency and shape of the quench signal, and their expressions can be found in [3]. In particular, K can be calculated through

$$K = K_0 K_s \zeta_0 \omega_0 \int_{t_a}^{t_b} p_b(t) s(t) dt \quad (5)$$

where K_s is the superregenerative gain, which is associated with

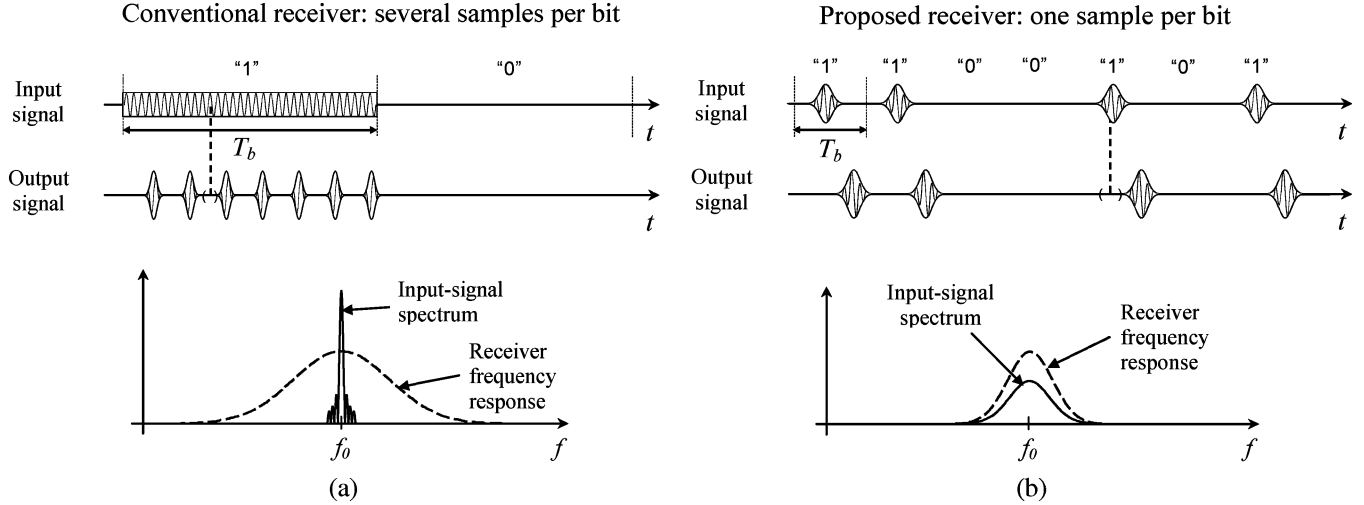


Fig. 2. Time and frequency diagrams representing the SRO input and output signals with OOK modulation. (a) Taking several samples per bit (classical receiver). (b) Taking one sample per bit (implemented receiver).

an exponential buildup of the oscillation

$$K_s = e^{-\omega_0 \int_0^{t_b} \zeta(\lambda) d\lambda} \quad (6)$$

and $s(t)$ is the sensitivity curve, a normalized function that takes the maximum of unity at $t = 0$ [3]

$$s(t) = e^{\omega_0 \int_0^t \zeta(\lambda) d\lambda} \approx e^{-\frac{1}{2} \left(\frac{t}{\sigma_s}\right)^2}. \quad (7)$$

When the slope of $\zeta(t)$ at $t = 0$ is finite, $s(t)$ can be approximated by a Gaussian function, as expressed in (7), whose standard deviation σ_s is considerably smaller than the quench period. Simulation carried out in [18] predicts $0.03T_q < \sigma_s < 0.15T_q$ for normal conditions of operation. Consequently, (5) shows that the receiver is especially sensitive to the input signal in a certain environment at the instant $t = 0$, which is called the sensitivity period. This point confirms the behavior of the SRO as a sampling device. The RF bandwidth of the receiver is proven to be inversely proportional to σ_s , in accordance with [3], [18]

$$\Delta f_{-3\text{dB}} = \frac{\sqrt{\ln 2}}{\pi} \frac{1}{\sigma_s}. \quad (8)$$

Fig. 2(a) illustrates operation in the linear mode of a conventional receiver with a narrowband on-off keying (OOK) modulated input signal. The SRO is asynchronously quenched several times during each bit period T_b to satisfy the Nyquist criterion so that the information can be retrieved by low-pass filtering the baseband bit samples. As shown in Fig. 2(a), since the sensitivity period is much shorter than the bit period, the resulting RF bandwidth is much greater than the modulation bandwidth. Roughly, $\sigma_s \ll T_q \ll T_b$; therefore, $\Delta f_{-3\text{dB}} \gg f_b = 1/T_b$. This is the main reason why this receiver exhibits poor selectivity.

III. SYNCHRONOUS OPERATION OF THE RECEIVER

Fig. 2(b) illustrates the mode of operation employed in the current receiver for detecting OOK-modulated signals.

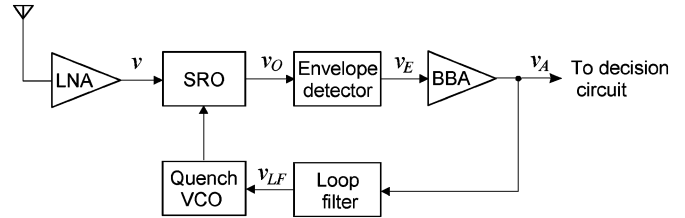


Fig. 3. Block diagram of the synchronous superregenerative receiver.

The SRO is quenched synchronously with the received signal so that a single sample of each bit pulse is taken. The synchronous operation of the SRO has already been exploited in spread-spectrum communications. However, unlike the architectures described in [14], in which the input signal is sampled at a rate of one sample per chip with subsequent integration of the chip samples to retrieve the bit values, in the current approach, the bits are sampled directly. This means that the quench frequency equals the bit frequency. Since the duration of the sampled bit is closer to that of the sensitivity period, the bandwidth of the modulated signal and that of the receiver become similar. Moreover, the synchronous operation allows the use of special bit envelopes that concentrate the signal energy in the sensitivity periods. In particular, (5) indicates that the receiver operates as a matched filter when the signal envelope matches the sensitivity curve, i.e., when $p_b(t) = s(t)$. In this way, the receiver can make more efficient use of the incoming signal power.

The block diagram of the receiver is shown in Fig. 3. It incorporates a PLL that controls the quench voltage-controlled oscillator (VCO) to ensure bit sampling is properly carried out. The error signal is obtained from the output of the envelope detector, which is passed through a baseband amplifier (BBA) and a loop filter. Fig. 4 shows the normalized envelope of the received bit pulse and the sensitivity curve of the SRO under normal operation. Once acquisition has been achieved, the loop performs tracking by centering the sensitive periods of the SRO on the

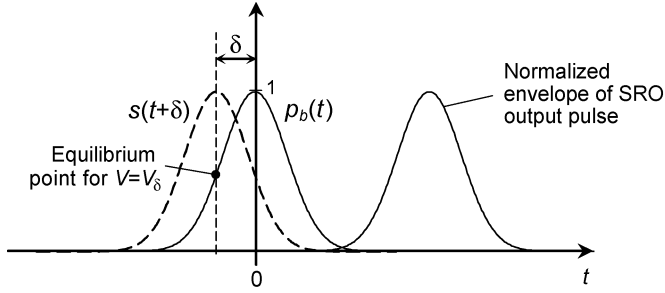


Fig. 4. Normalized envelope of the input bit pulse $p_b(t)$, shifted sensitivity curve of the SRO $s(t + \delta)$, and normalized envelope of the SRO output oscillation.

ascending flanks of the bit pulses received. Thus, the phase deviation of the quench VCO with regard to the received pulse results in an amplitude variation at the loop-filter output that tends to correct the error. Operation on a single flank allows a simpler architecture to be implemented.

IV. USE OF THE SRO AS A PHASE DETECTOR

The classical theory of PLLs is applicable to the current design. The main novelty in this scheme is in the way in which the phase is detected by the SRO. Proper PLL performance requires that the sensitive periods of the SRO be centered on the rising flanks of the bit envelopes, which means that a certain tracking error δ must exist for a given input-signal amplitude V_δ when the input bit frequency f_b is locked (Fig. 4). From (4) and (5), the incremental voltage of a tuned receiver at the envelope detector output when the sensitivity curve is delayed t_d s with respect to the equilibrium point in Fig. 4, as well as for a generic peak amplitude V of the input bit pulse, is defined by

$$\Delta v_E = V K_0 K_s \zeta_0 \omega_0 p(t) D(t_d, V) \quad (9)$$

where the function $p(t)$ is subsequently averaged by the loop filter and $D(t_d, V)$ provides the discrimination characteristic

$$D(t_d, V) = R_{pbs}(t_d - \delta) - \frac{V_\delta}{V} R_{pbs}(-\delta). \quad (10)$$

$R_{pbs}(\tau)$ is the cross-correlation of $p_b(t)$ (normalized bit envelope) and $s(t)$ (sensitivity curve of the SRO).

As has been mentioned, a return-to-zero bit envelope matched to the sensitivity curve of the SRO ($p_b(t) = s(t)$) is optimum for the SRO. Assuming this condition and also the Gaussian expression of $s(t)$ (7), the expression of the discrimination characteristic becomes

$$D(t_d, V) = \sqrt{\pi} \sigma_s \left(e^{-\frac{1}{2} \left(\frac{t_d - \delta}{\sqrt{2} \sigma_s} \right)^2} - \frac{V_\delta}{V} e^{-\frac{1}{2} \left(\frac{\delta}{\sqrt{2} \sigma_s} \right)^2} \right). \quad (11)$$

Fig. 5 shows the normalized discrimination curves for several values of δ with $V = V_\delta$, where the origin corresponds to a stable equilibrium point of operation. Generally, as is confirmed in practice, the best performance from the point of view of tracking occurs when δ is approximately $1.7 \sigma_s$, as it provides a linear behavior with a larger dynamic range around the origin. However, a smaller value may be preferred in order to increase the output signal-to-noise ratio, especially at low signal levels

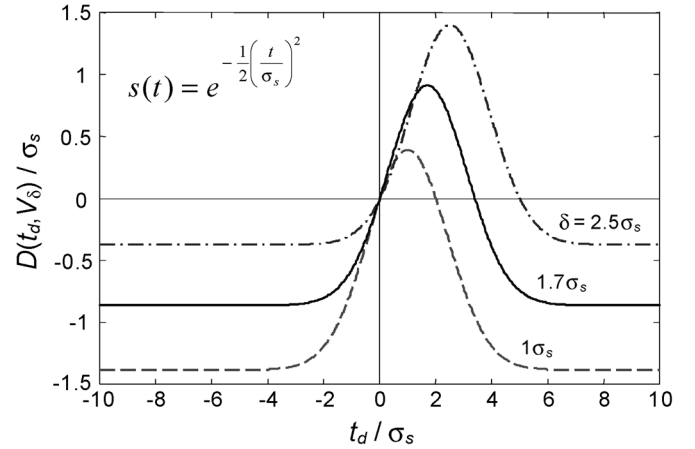


Fig. 5. Normalized discrimination characteristic for several values of δ and $V = V_\delta$.

(ideally, $\delta = 0$ from the point of view of data detection). Therefore, a compromise must be established in practice.

V. DESCRIPTION OF THE IMPLEMENTED PROTOTYPE

A schematic diagram of the implemented receiver is shown in Fig. 6. It is a discrete-element prototype based on the diagram in Fig. 3 and built on a printed circuit board (PCB) with a 0.8-mm FR-4 substrate.

The RF part (LNA, SRO, and envelope detector) is based on the design presented in [17], which was developed and electromagnetically simulated with Agilent Technologies' Advanced Design System (ADS). The BFP405 transistor is used in the RF stages to take advantage of its high gain at low biasing currents and low parasitic capacitances. The LNA is a cascode configuration providing high reverse isolation of approximately 38 dB. It includes an input matching network to achieve a minimum noise figure below 3 dB. The SRO is built on a Colpitts oscillator operating at 2.45 GHz, in which the inductance is provided by a small microstrip line. The quench is applied through the base by means of an RF choke to avoid oscillator loading effects. The LNA and the envelope detector are connected to the SRO transistor base to take advantage of higher signal amplitude. The impedance of the choke and of the inter-stage capacitors is carefully chosen to avoid unwanted filtering of the quench signal at high quench frequencies. The resonance frequency of the loaded SRO is adjustable around 2.45 GHz, and the quiescent loaded Q , when the quench is disabled, equals 38. This value is the result of a compromise between achieving high quench frequencies and low current consumption. The envelope detector is built on a common-collector configuration in which the emitter capacitor is charged by the transistor and discharged through the emitter resistor. It includes a filter in the biasing network to remove the quench components transferred from the SRO. Limited by the cascode, the minimum supply voltage of this architecture is approximately 0.95 V. Further details on the RF part are described in [17].

The BBA makes use of a common-emitter inverting amplifier to increase the amplitude provided by the envelope detector from approximately 50 mVpp to 0.5 Vpp on an output load of

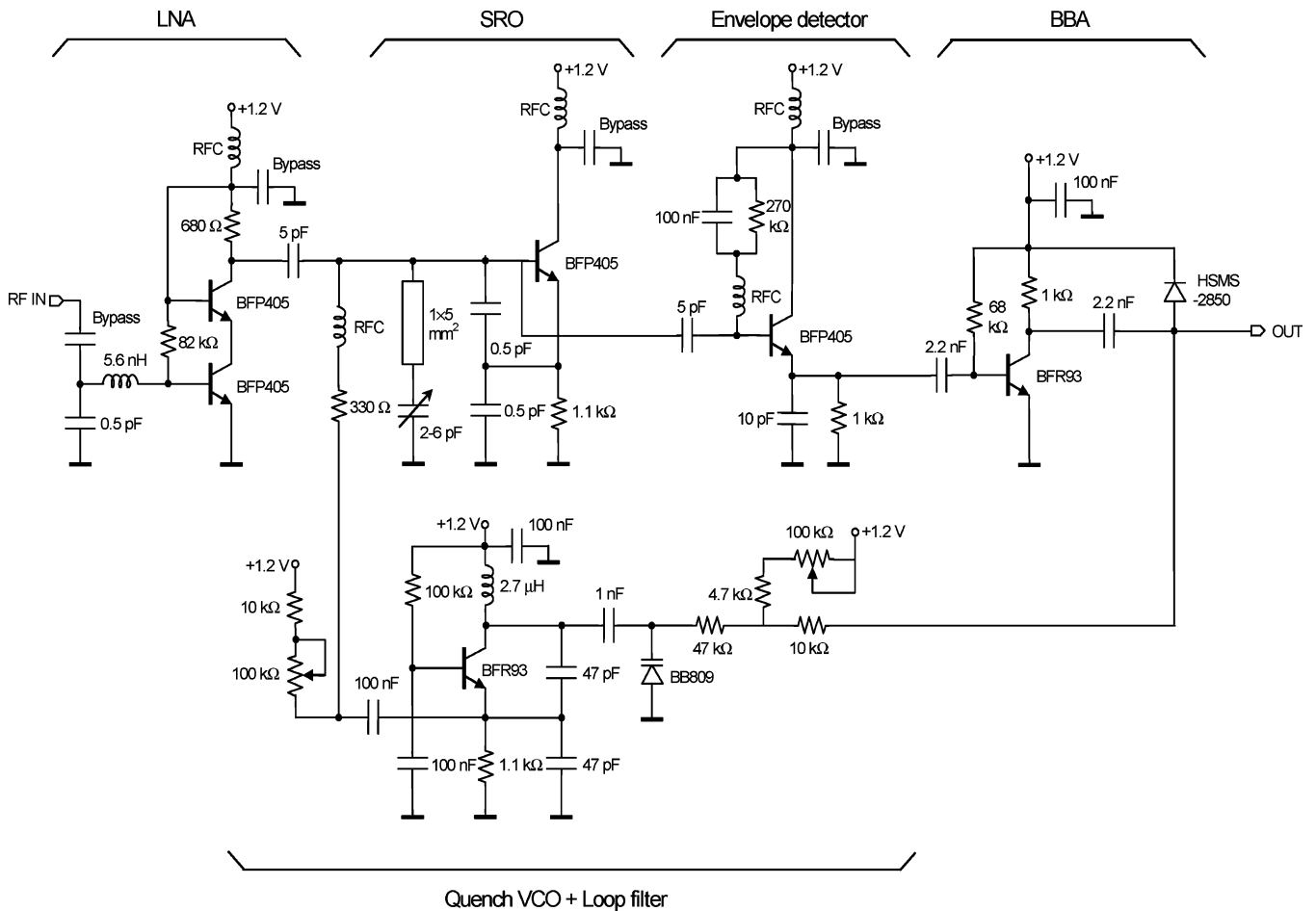


Fig. 6. Complete schematic of the implemented receiver (11-Mb/s data rate).

10 pF. A clamper is included at the output to restore the upper base line of the signal. The output pulses can be used directly to perform the data detection and, unlike classical receivers, no low-pass filter is required to integrate the bit samples and remove the quench components.

A common-base Colpitts oscillator acts as the quench VCO, in which a resistive feedback network and the coupling capacitor of the varicap act as a first-order loop filter. The quench signal generated is sinusoidal and has a relatively small amplitude, which ensures that a more selective receiver is obtained. The quench signal is taken from the emitter because of the low output impedance in this node. The signal inversion caused by the BBA amplifier means that the PLL leads the SRO to operate on the descending flank of the received pulses instead of the ascending one (Fig. 4).

A modified version of the scheme in Fig. 6 adapted to operate at a lower rate of 1 Mb/s was also evaluated.

VI. EXPERIMENTAL RESULTS

The performance of the architecture presented was evaluated at 1- and 11-Mb/s data rates. Fig. 7 shows a sequence of the modulating signal and the corresponding voltages measured at the receiver side at 11 Mb/s. Fig. 8 shows the frequency selectivity curves at 1 and 11 Mb/s and Table I summarizes the receiver’s main features. The signal modulation was, in all cases, an OOK modulation with a matched Gaussian bit envelope to

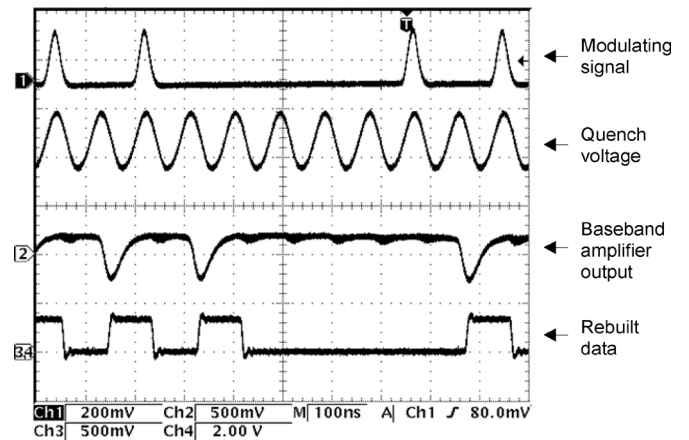


Fig. 7. Signals at the transmitter and receiver sides at 11-Mb/s data rate.

improve sensitivity and facilitate PLL operation. The selectivity curves were obtained from the rejection of a continuous wave (CW) signal with regard to the reception center frequency. The -3 -dB bandwidth is 5 and 38 MHz, respectively. Note that the ratio between the receiver RF bandwidth and the data rate is much smaller than in a classical receiver. For instance, a classical receiver operating at 1 Mb/s and taking ten samples per bit would require a quench frequency of 10 MHz, thus exhibiting a bandwidth close to 38 MHz. With the synchronous operation,

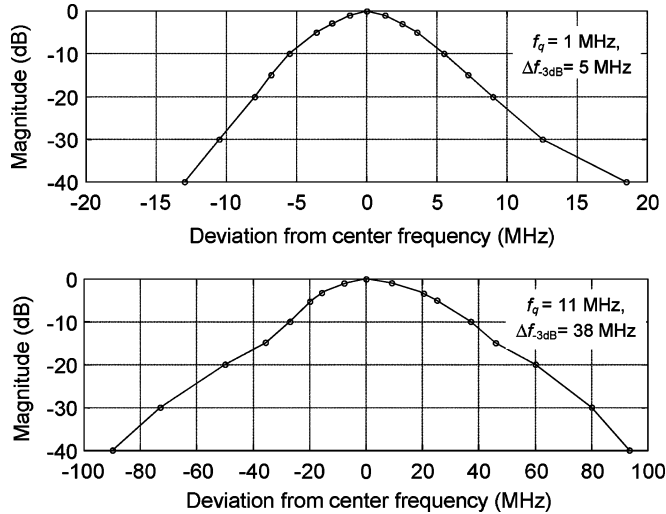


Fig. 8. Selectivity curves at 1- and 11-MHz quench frequency.

TABLE I
SUMMARY OF RECEIVER PERFORMANCE

Parameter	1-Mb/s data rate	11-Mb/s data rate	Unit
Supply voltage	1.2		V
Reception center frequency	2.45		GHz
Signal modulation	OOK, Gaussian bit envelope		
Quench waveshape	Sinusoidal		
-3 dB bandwidth	5	38	MHz
Sensitivity level (BER=10 ⁻³)	-92	-81	dBm
Peak-to-peak output voltage at sensitivity level (10 pF load)	0.5	0.5	V
Typical PLL pull-in / hold-in range (RF input level = 10 dB above sensitivity level)	1.5 / 2.7	20 / 38	kHz
Input-signal dynamic range	45 - 65	16 - 40	dB
Input-referred IP3	-23	-12	dBm
Leaked power at the antenna (10-MHz bandwidth)	< -67	< -63	dBm
Total power consumption	1.1	2.1	mW

the RF bandwidth is only 5 MHz. At 11 Mb/s, the ratio between the RF bandwidth and the data rate, which is equal to 3.5, is even more favorable. In comparison with a Bluetooth receiver, the current prototype at 1 Mb/s turns out to be less selective [19]. However, the use of a matched modulation consisting of a bit envelope with relatively small duty cycle will generally introduce additional rejection to both adjacent channel and cochannel interference.

A characteristic of the implemented receiver is that the demodulated output becomes independent from the input signal level within a certain range. The reason for this is that the loop advances or delays the phase of the quench VCO to regulate the amount of input signal power that falls into the sensitivity pe-

TABLE II
DISTRIBUTION OF THE CURRENT CONSUMPTION IN THE RECEIVER IN MICROAMPERES

Block	1-Mb/s data rate	11-Mb/s data rate
LNA	410	410
SRO	180	420
Envelope detector	110	110
Quench VCO + loop filter	140	290
BBA	70	520
TOTAL	910	1750

TABLE III
COMPARISON OF SUPERREGENERATIVE RECEIVER PERFORMANCE

	[1]	[4]	[6]	This work
Operating frequency	1 GHz	1.9 GHz	2.4 GHz	2.4 GHz
Data rate	100 kb/s	5 kb/s	500 kb/s	11 Mb/s
Sensitivity (BER=10 ⁻³) @ 1.2 kb/s	-107.5 dBm	-100.5 dBm	-80 dBm	-81 dBm
Power consumption	1.2 mW	0.4 mW	2.8 mW	2.1 mW
Energy per bit	12 nJ/bit	80 nJ/bit	5.6 nJ/bit	0.19 nJ/bit

riods of the SRO. This ensures that, in the steady state of operation, the control signal of the VCO exhibits a fixed level to maintain the loop in lock. This self-regulation mechanism acts as an automatic level control. The supported input dynamic range depends in practice on the characteristics and adjustment of the loop filter.

Table II shows the distribution of consumption in the receiver and Table III compares the implemented receiver with other reported superregenerative architectures. The data rate achieved by the current prototype exceeds that of previous designs by more than one order of magnitude, and the energy per received bit is substantially lower. Its sensitivity is also remarkable in comparison with the data rate. The net sensitivity improvement due to the use of a matched bit envelope taking into account the tracking error of the PLL is in the order of 7 dB.

Finally, we mention that the implemented SRO can be operated at higher data rates (nearly 18 Mb/s). However, sensitivity decreases progressively due to hangover limitations [3].

VII. CONCLUSION

In this paper, a high-performance superregenerative receiver has been presented that allows the limits of superregeneration in the ISM band of 2.4 GHz to be assessed. The receiver uses a moderate resonator Q to support high quench frequencies and operates in a synchronous mode, the latter yielding a significant number of advantages as follows.

- 1) *Increased data rate*: since this rate equals the quench frequency and not a fraction of it. In particular, 11 Mb/s is

a landmark value for this type of receiver that clearly surpasses previously reported values [1]–[7].

- 2) *Improved selectivity*: the RF bandwidth of the receiver is much closer to the bandwidth of the received signal, overcoming one of the traditional drawbacks of the receiver.
- 3) *Improved sensitivity*: the use of a matched bit envelope allows the bit energy to be concentrated in the sensitivity periods of the receiver. The improvement typically ranges from 5 to 10 dB.
- 4) *Simplicity*: since each received bit can be detected in a single quench period, the synchronous receiver does not require the relatively high-order low-pass filter that is commonly included in conventional receivers to remove quench components.
- 5) *Reduced power consumption*: for a given data rate, the receiver can be quenched at a lower frequency, which reduces current consumption in the SRO.
- 6) *Data clock*: the quench signal can be used as a bit-synchronous clock reference in subsequent circuits, which renders additional clock recovery circuits unnecessary.

In summary, the current design demonstrates that superregenerative receivers can be successfully operated in the 2.4-GHz ISM band with an outstanding tradeoff between cost, performance, and power consumption. The synchronous operation is also applicable to high- Q SROs operating at low data rates.

REFERENCES

- [1] A. Vouilloz, M. Declercq, and C. Dehollain, "A low power CMOS super-regenerative receiver at 1 GHz," *IEEE J. Solid-State Circuits*, vol. 36, no. 3, pp. 440–451, Mar. 2001.
- [2] N. Joehl, C. Dehollain, P. Favre, P. Deval, and M. Declercq, "A low power 1 GHz super-regenerative transceiver with time-shared PLL control," *IEEE J. Solid-State Circuits*, vol. 36, no. 7, pp. 1025–1031, Jul. 2001.
- [3] F. X. Moncunill-Geniz, P. Palà-Schönwälder, and O. Mas-Casals, "A generic approach to the theory of superregenerative reception," *IEEE Trans. Circuits Syst. I, Reg. Papers*, vol. 52, no. 1, pp. 54–70, Jan. 2005.
- [4] B. Otis, Y. H. Chee, and Y. Rabaey, "A 400 μ W-RX, 1.6 mW-TX super-regenerative transceiver for wireless sensor networks," in *IEEE Int. Solid-State Circuits Conf. Tech. Dig.*, San Francisco, CA, Feb. 2005, vol. 1, pp. 396–397, 606.
- [5] J. Y. Chen, M. P. Flynn, and J. P. Hayes, "A 3.6 mW 2.4-GHz multi-channel super-regenerative receiver in 130 nm CMOS," *Proc. IEEE Custom Integrated Circuits Conf.*, pp. 361–364, Sep. 2005.
- [6] J. Y. Chen, M. P. Flynn, and J. P. Hayes, "A fully integrated auto-calibrated superregenerative receiver," in *IEEE Int. Solid-State Circuits Conf. Tech. Dig.*, Feb. 2006, pp. 1490–1499.
- [7] I. McGregor, G. Whyte, K. Elgaid, E. Wasige, and I. Thayne, "A 400 μ W Tx/380 μ W Rx 2.4 GHz super-regenerative GaAs transceiver," in *Proc. 36th Eur. Microw. Conf.*, Manchester, U.K., Sep. 2006, pp. 1523–1525.
- [8] V. Leibman, "Superregenerative low-power receiver," W.O. Patent 03 009 482, Jan. 30, 2003.
- [9] K. L. Addy, "Thermostat having a temperature stabilized super-regenerative RF receiver," U.S. Patent 6 810 307, Oct. 26, 2004.
- [10] G. M. Vavik, "Transponder, including transponder system," U.S. Patent 2005/0 270 222, Dec. 8, 2005.
- [11] E. H. Armstrong, "Some recent developments of regenerative circuits," *Proc. IRE*, vol. 10, no. 8, pp. 244–260, Aug. 1922.
- [12] W. R. Day, "Superregenerative backward wave amplifiers for millimeter waves," *Proc. IEEE*, vol. 52, no. 6, pp. 711–712, Jun. 1964.
- [13] N. B. Buchanan, V. F. Fusco, and J. A. C. Stewart, "A K_a band MMIC super regenerative detector," in *IEEE MTT-S Int. Microw. Symp. Dig.*, Jun. 2000, vol. 3, pp. 1585–1588.

- [14] F. X. Moncunill-Geniz, P. Palà-Schönwälder, and F. del Águila-Lopez, "New superregenerative architectures for direct-sequence spread-spectrum communications," *IEEE Trans. Circuits Syst. II, Exp. Briefs*, vol. 52, no. 7, pp. 415–419, Jul. 2005.
- [15] F. X. Moncunill-Geniz, P. Palà-Schönwälder, C. Dehollain, N. Joehl, and M. Declercq, "A 2.4-GHz DSSS superregenerative receiver with a simple delay-locked loop," *IEEE Microw. Wireless Compon. Lett.*, vol. 15, no. 8, pp. 499–501, Aug. 2005.
- [16] D. L. Ash, "A low cost superregenerative SAW stabilized receiver," *IEEE Trans. Consumer Electron.*, vol. CE-33, no. 3, pp. 395–403, Aug. 1987.
- [17] F. X. Moncunill-Geniz, C. Dehollain, N. Joehl, M. Declercq, and P. Palà-Schönwälder, "A 2.4-GHz low-power superregenerative RF front-end for high data rate applications," in *Proc. 36th Eur. Microw. Conf.*, Manchester, U.K., Sep. 2006, pp. 1537–1540.
- [18] F. X. Moncunill Geniz, "New super-regenerative architectures for direct-sequence spread-spectrum communications," Ph.D. dissertation, Dept. Signal Theory Commun., Univ. Politècnica Catalunya, Barcelona, Spain, 2002.
- [19] H. A. Alzahrer and M. K. Alghamdi, "A CMOS bandpass filter for low-IF Bluetooth receivers," *IEEE Trans. Circuits Syst. I, Reg. Papers*, vol. 53, no. 8, pp. 1636–1647, Aug. 2006.



F. Xavier Moncunill-Geniz received the Telecommunications Engineering and Ph.D. degrees from the Technical University of Catalonia, Barcelona, Spain, in 1992 and 2002, respectively.

He is currently a Collaborating Professor with the Department of Signal Theory and Communications, School of Telecommunications Engineering of Barcelona (ETSETB), Technical University of Catalonia, where he is involved in the field of circuit theory and analog electronics. His main research area is RF circuit design with a particular emphasis on

the theory and implementation of new superregenerative receiver architectures.



Pere Palà-Schönwälder (S'89–A'95–M'05) received the Telecommunications Engineering and Ph.D. degrees from the Technical University of Catalonia, Barcelona, Spain, in 1989 and 1994, respectively.

He is currently an Associate Professor with the Department of Signal Theory and Communications, School of Engineering of Manresa (EPSEM), Technical University of Catalonia. He has managed several Spanish research projects. His research interests include computer-aided circuit design,

nonlinear circuits, and RF communication electronics.



Catherine Dehollain (M'93) received the M.Sc. degree in electrical engineering and Ph.D. degree from the Swiss Federal Institute of Technology (EPFL), Lausanne, Switzerland, in 1982 and 1995, respectively.

Since 1995, she has been with the Electronics Laboratory (LEG), EPFL, where she is responsible for RF activities. Since 1998, she has been a Lecturer with the EPFL in the area of RF circuits, electric filters and computer-aided design (CAD) tools.

Since 2006, she has been Maître d'Enseignement et de Recherche (MER) with the EPFL. She has authored or coauthored four scientific books and 50 scientific publications. Her research interests include low-power analog circuits and electric filters.



Norbert Joehl was born in Geneva, Switzerland, in 1959. He received the M.S. and Ph.D. degrees in electrical engineering from the Swiss Federal Institute of Technology (EPFL), Lausanne, Switzerland, in 1985 and 1992, respectively.

Since 1985, he has been with the Electronics Laboratory, EPFL, where he has been involved in the field of low-power and high-performance RF analog CMOS and BiCMOS integrated circuit design and is currently responsible for research activities. He was a Lecturer of electronic systems with the École

d'Ingénieurs de l'Etat de Vaud. He has authored or coauthored approximately 20 scientific publications.



Michel Declercq (S'70–M'72–SM'97–F'00) received the Electrical Engineering degree and Ph.D. degree from the Catholic University of Louvain, Louvain, Belgium, in 1967 and 1971, respectively.

In 1985, he joined the Swiss Federal Institute of Technology (EPFL), Lausanne, Switzerland, where he is currently a Professor, Dean of the School of Engineering, and Director of the Electronics Laboratory. He is an Expert of the European Commission for scientific research programs in information technologies. He has authored or coauthored over 220 sci-

entific publications and three books. He holds several patents. His research activities are related to mixed analog-digital integrated-circuit design and design methodologies.